

# Side-chain to backbone correlations from solid-state NMR of perdeuterated proteins through combined excitation and long-range magnetization transfers

Rasmus Linser

Received: 27 March 2011 / Accepted: 11 July 2011 / Published online: 7 August 2011  
© Springer Science+Business Media B.V. 2011

**Abstract** Proteins with excessive deuteration give access to proton detected solid-state NMR spectra of extraordinary resolution and sensitivity. The high spectral quality achieved after partial proton back-exchange has been shown to start a new era for backbone assignment, protein structure elucidation, characterization of protein dynamics, and access to protein parts undergoing motion. The large absence of protons at non-exchangeable sites, however, poses a serious hurdle for characterization of side chains, which play an important role especially for structural understanding of the protein core and the investigation of protein–protein and protein–ligand interactions, e.g. This has caused the perdeuteration approach to almost exclusively be amenable to backbone characterization only. In this work it is shown that a combination of isotropic  $^{13}\text{C}$  mixing with long-range  $^1\text{H}/^{13}\text{C}$  magnetization transfers can be used effectively to also access complete sets of side-chain chemical shifts in perdeuterated proteins and correlate these with the protein backbone with high unambiguity and resolution. *COMBINED POLARIZATION FROM LONG-RANGE TRANSFERS AND DIRECT EXCITATION (COPORADE)* allows this strategy to yield complete sets of aliphatic amino acid resonances with reasonable sensitivity.

**Keywords** MAS solid-state NMR · Magic Angle Spinning · Perdeuteration · Proton detection · TOBSY · Side-chain assignment · Micro-crystalline proteins

**Electronic supplementary material** The online version of this article (doi:10.1007/s10858-011-9531-3) contains supplementary material, which is available to authorized users.

R. Linser (✉)  
Analytical Centre and School of Chemistry, University of New South Wales, Sydney, NSW 2052, Australia  
e-mail: r.linser@unsw.edu.au

## Introduction

Understanding the functions of a particular protein is usually approached via its three-dimensional backbone fold. Its mode of action, however, strongly depends on the interplay of the single amino acid side chains and their individual chemical behaviour. Aliphatic side chains, for example, present a valuable probe for the assessment of parameters like protein dynamics (Sprangers and Kay 2008) or intermolecular interactions (Velyvis et al. 2009). Traditional solid-state NMR spectroscopy focuses on protonated proteins and has recently become a popular means for characterization of their structure and dynamics. Using this approach, spectroscopic data for side-chain carbons are straightforward to obtain and form an ordinary first step towards structure elucidation. (Castellani et al. 2002; Petkova et al. 2002; Lange et al. 2006; Loquet et al. 2008; Wasmer et al. 2008; Cady et al. 2010). A recent strategy, on the other hand, is based on protein perdeuteration and only partial back-exchange of deuterons for protons. (Morcombe et al. 2005; Chevelkov et al. 2006; Linser et al. 2011b). This approach has been shown to yield far superior spectral resolution due to the absence of strong  $^1\text{H}$  dipolar interactions (McDermott et al. 1992; Tang et al. 2010), allowing for extremely long-lived spin states (Linser et al. 2008; Schanda et al. 2009; Linser et al. 2010b), avoiding rf-induced sample heating (Linser et al. 2007), and giving access to unperturbed, site-resolved relaxation parameters (Chevelkov et al. 2009; Linser et al. 2009; Schanda et al. 2010) and proton–proton long-range distances based structure elucidation (Linser et al. 2011a). For perdeuterated proteins, however, side-chain protons are largely absent and cannot be used for magnetization transfer to the side-chain carbon nuclei. Ordinary direct excitation of  $^{13}\text{C}$ , on the other hand, is compromised by long  $T_1$  and a

comparably low gyromagnetic ratio. These drawbacks make side-chain resonances appear inaccessible for solid-state NMR of perdeuterated samples. Despite its great potential, this technique has thus been employed only to gather additional information to already well understood systems so far.

In this work a strategy is presented that yields highly resolved correlations between the complete set of side-chain carbons and the protein backbone (Side-chain to Backbone-correlations, called *S2B* in the following). Yielding chemical shifts of up to eight covalently bonded atoms per strip, this approach represents one of the most comprehensive intraresidual solid-state NMR correlation experiments obtainable so far.

## Materials and methods

All spectra were recorded using approximately 6 mg SH3 domain of uniformly  $^2\text{H}$ ,  $^{15}\text{N}$ ,  $^{13}\text{C}$ -labelled chicken  $\alpha$ -spectrin, which was expressed and purified as described earlier (Linser et al. 2007). Micro-crystallization was pursued in a buffer containing 75%  $\text{D}_2\text{O}$  and 25%  $\text{H}_2\text{O}$  as well as 75 mM  $(\text{NH}_4)_2[\text{Cu}(\text{edta})]$  by pH shift from 3.5 to 7.5. The material was center-packed into a 2.5 mm rotor using compressed Teflon<sup>®</sup> tape in the bottom and top part of the rotor. NMR experiments were carried out at 700 MHz proton Larmor frequency, 25 kHz MAS, and an effective temperature of 25°C using a 2.5 mm triple-resonance probe on a Bruker Avance III spectrometer. CP contact times of 4 ms, 280  $\mu\text{s}$ , and 3 ms and effective fields of 85 kHz/50 kHz (70–100% ramp on  $^1\text{H}$ ), 20 kHz/43 kHz (70–100% ramp on  $^{15}\text{N}$ ), and 35 kHz/50 kHz (70–100% ramp on  $^{13}\text{C}$ ) were used for  $^1\text{H}/^{13}\text{C}$ ,  $^1\text{H}/^{15}\text{N}$ , and  $^{13}\text{C}/^{15}\text{N}$  transfers, respectively. Decoupling fields amounted to 4 kHz on  $^{15}\text{N}$  and 7 kHz on  $^1\text{H}$ . Recycle delays were set to 1.8 s. TOBSY (Baldus and Meier 1996; Leppert et al. 2004) was implemented as described by Agarwal et al. (Agarwal and Reif 2008), optimising the pulse duration around 32  $\mu\text{s}$  for an effective field of 37 kHz and 16 ms total duration.

Data processing, chemical shift assignment, read-out of intensities, and preparation of figures was performed using Bruker Topspin, Sparky (Goddard and Kneller 2004), and CcpNmr Analysis software (Vranken et al. 2005).

## Results and discussion

The suggested strategy is represented in Fig. 1. Figure 1b, c show representative total side-chain correlation strips from the 3D experiment for amide chemical shifts of this residue and in addition for a random Thr, Gln, and Leu-residue (T24, Q16, and L61), put into context by a

comparison to HNCA/HNCACB experiments. The approach, which is represented schematically in Fig. 1a, is based on a combination of direct carbon excitation and long-range magnetization transfer from protons, (Agarwal et al. 2010b) which are present only at exchangeable sites and, to a small amount, at methyl groups due to a residual protonation of deuterated glucose (Agarwal and Reif 2008). This is coined *COPORADE* (COMBINED POLARIZATION from long-RANGE transfers AND Direct EXCITATION) here. Long-range  $^{13}\text{C}$ - $^1\text{H}$  magnetization transfers are further used to correlate side-chain chemical shifts with the amide backbone (see below). In order to further enhance correlations with distant side-chain carbons, isotropic homonuclear mixing using TOBSY (Baldus and Meier 1996; Leppert et al. 2004) is employed. A pulse scheme is shown in Fig. 3.

*COPORADE* effectively overcomes the problem of obtaining sufficient polarization for  $^{13}\text{C}$  side-chain resonances in the absence of side-chain protons. The traditional approach of generating  $^{13}\text{C}$  magnetization through Cross Polarization (CP) does provide a certain degree of transferred polarization from distant protons into the side chain (compare Supplementary Figure 5). However, especially for nuclei far apart from non-mobile partially back-exchanged protons, as found in Lys-residues etc., the Cross Polarization obtained is weak.

For  $^{13}\text{C}$  nuclei distant from protons, direct excitation yields a much higher starting magnetization (see Supplementary Figure 5). Since  $^{13}\text{C}$   $T_1$  times can be relatively long, Paramagnetic Relaxation Enhancement (PRE) (Linser et al. 2007; Wickramasinghe et al. 2007) by EDTA-chelated  $\text{Cu}^{\text{II}}$  can be employed to enhance  $^{13}\text{C}$  longitudinal relaxation. Although this strategy may potentially interfere with micro-crystallisation, it has been found to be unproblematic for the sample preparation of several micro-crystalline, amyloidic, and membrane proteins in our hands. (Linser et al. 2011b) The bulk  $T_1$  for  $^{13}\text{C}^\alpha$  and  $^{13}\text{CO}$ , affected by 75 mM  $[\text{Cu}(\text{edta})]^{2-}$ , was measured to be approximately 1.6 and 1.4 s, respectively (see Supplementary Figure 2). This decreases the recycle delay to around 1.8 s, which almost resembles the recycling rate usually used for solid-state NMR on protonated proteins. The *COPORADE* approach uses an additional long-range Cross Polarization (Agarwal et al. 2010b) from protons in addition to the polarization obtained by direct  $^{13}\text{C}$  excitation. The excited  $^{13}\text{C}$  magnetization is thereby spin locked and thus maintained during Hartmann-Hahn matching. Therefore, the CP spin lock is applied with respect to the excitation pulse (maintaining a 90° phase shift), which requires parallel phase changes for the whole excitation block for phase cycling and TPPI. Depending on the length of the CP and rf-field homogeneity, most of the original magnetization is maintained during  $T_{1\rho}$ -decay, and

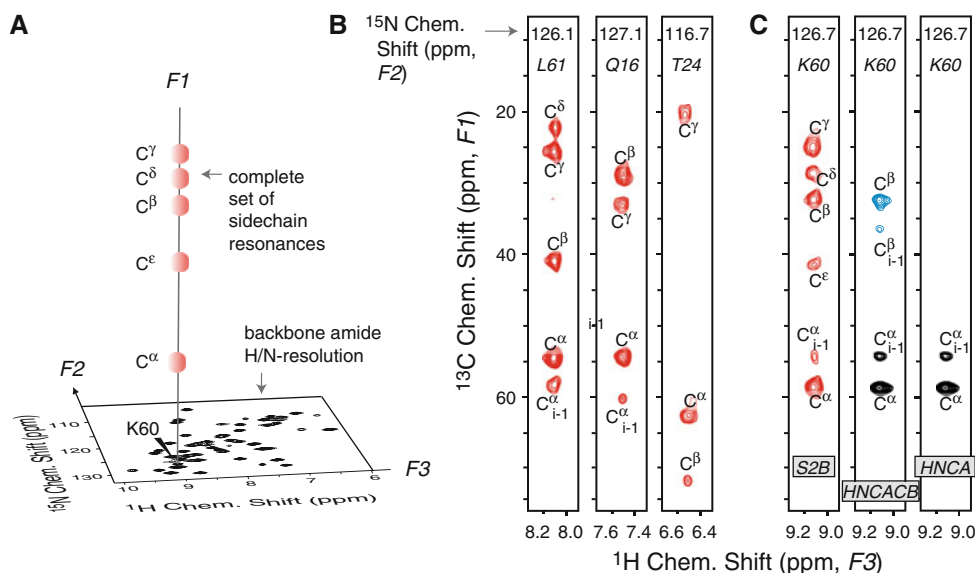


**Fig. 1** The *S2B* (Side-chain to Backbone) experiment correlates the complete set of  $^{13}\text{C}$  side-chain chemical shifts to the amide group of the protein backbone. **a** Pictorial representation of the correlations based on the amide- $^1\text{H}$  chemical shifts of the desired  $^{13}\text{C}$  resonance set in *F2* and *F3*, shown for lysine K60. **b** Representative set of *S2B* strips showing total side-chain correlations for  $^1\text{H}$  and  $^{15}\text{N}$  chemical shifts, taken for a random Leu-, Gln-, and Thr-residue, respectively, from an experiment recorded within 3.5d using 40 scans and 48 and 84 increments in *f2* and *f1*, respectively. The achievable resolution in the  $^{13}\text{C}$  dimension with a triple-resonance probe is determined by

scalar  $^{13}\text{C}$ - $^{13}\text{C}$  and  $^2\text{H}$ - $^{13}\text{C}$  couplings. Lowest contour levels were taken at approximately 3.5 times the noise level, using multipliers of 1.1. **c** Comparison of the side-chain completeness obtained by the *S2B*-experiment in comparison to an equally sensitive HNCACB (Linser et al. 2011b) (black and blue used for positive and negative contours, respectively, see Supplementary Figure 1C for the respective pulse scheme) and an HNCA experiment, showing only the  $\text{C}^\alpha$  resonances of the HNCACB. In comparison to these experiments, the *S2B* yields a much higher content of information. All experiments were recorded under identical conditions

especially for carbons close to protons, it is overcompensated by the additionally transferred magnetization.

For a correlation involving all side-chain carbon cross peaks, a  $^{13}\text{C}$  polarization of equal and high intensity is desired. The distribution and amount of the effective  $^{13}\text{C}$  start magnetization is assessed in Fig. 2, comparing 2D side-chain  $^{13}\text{C}$  to backbone  $^1\text{H}$  correlations employing both contributions (A), with  $^{13}\text{C}$  excitation only (B), and with  $^1\text{H}$  excitation (and transfer) only (C), respectively. The distribution among accessed side-chain nuclei is comparable for A and B, however, the overall intensity is boosted by the incorporation of additional  $^1\text{H}$  magnetization. For C, many correlations are missing apart from  $\text{C}^\alpha$  and Ala  $\text{C}^\beta$ . All spectra were acquired back-to-back and recorded and displayed identically. Although the distribution of signal intensity among the side-chain carbons can only be accessed in the 2D spectra, the bulk signal, as obtained from the first increment of a 2D experiment, yields an almost twofold increase in s/n when compared with the  $^{13}\text{C}$  only excitation with a similar excitation profile. The first slices of 2D  $^{13}\text{C}/^1\text{H}$ -correlations are compared in Supplementary Figures 3 and 4.

Although alternate ways of introducing dilute protons in otherwise perdeuterated proteins have been proposed (Asami et al. 2010), exchange at labile sites has proven to

yield high-quality spectroscopic data. In particular, high resolution spectra can be obtained due to narrow  $^1\text{H}$  and  $^{15}\text{N}$  linewidths and the fact that essentially one peak per residue is obtained only. Accordingly, H/N-shifts have been used for resolving NMR signals in various kinds of correlation experiments representing a basis for assignment (Wittekind and Mueller 1993; Linser et al. 2008, 2010a), dynamics (Loria et al. 1999; Chevelkov et al. 2010; Schanda et al. 2010), protein surface accessibilities (Pintacuda and Otting 2002; Linser et al. 2009) etc. both in solution and in the solid state. With this in mind, side-chain carbon chemical shifts were encoded by their respective amide shifts, yielding a perfect resolution of side-chain shift information for a specific residue from that of other residues.

For an effective transfer of side-chain  $^{13}\text{C}$  magnetization to the backbone amide, the following strategy was developed. Rather than using a direct  $^{13}\text{C}$  to  $^{15}\text{N}$  transfer, a detour via amide protons in two successive CP steps turns out to be beneficial for complete *S2B* correlations (see Fig. 3). This has its justification in the need for long-range magnetization transfer from  $^{13}\text{C}$  nuclei very distant from the amide group.  $^{13}\text{C}/^1\text{H}$  long-range transfers have been shown to cross that distance, the reason being a higher gyromagnetic ratio of protons in comparison to  $^{15}\text{N}$ . (Agarwal et al. 2010a) Apart from the comparably slow

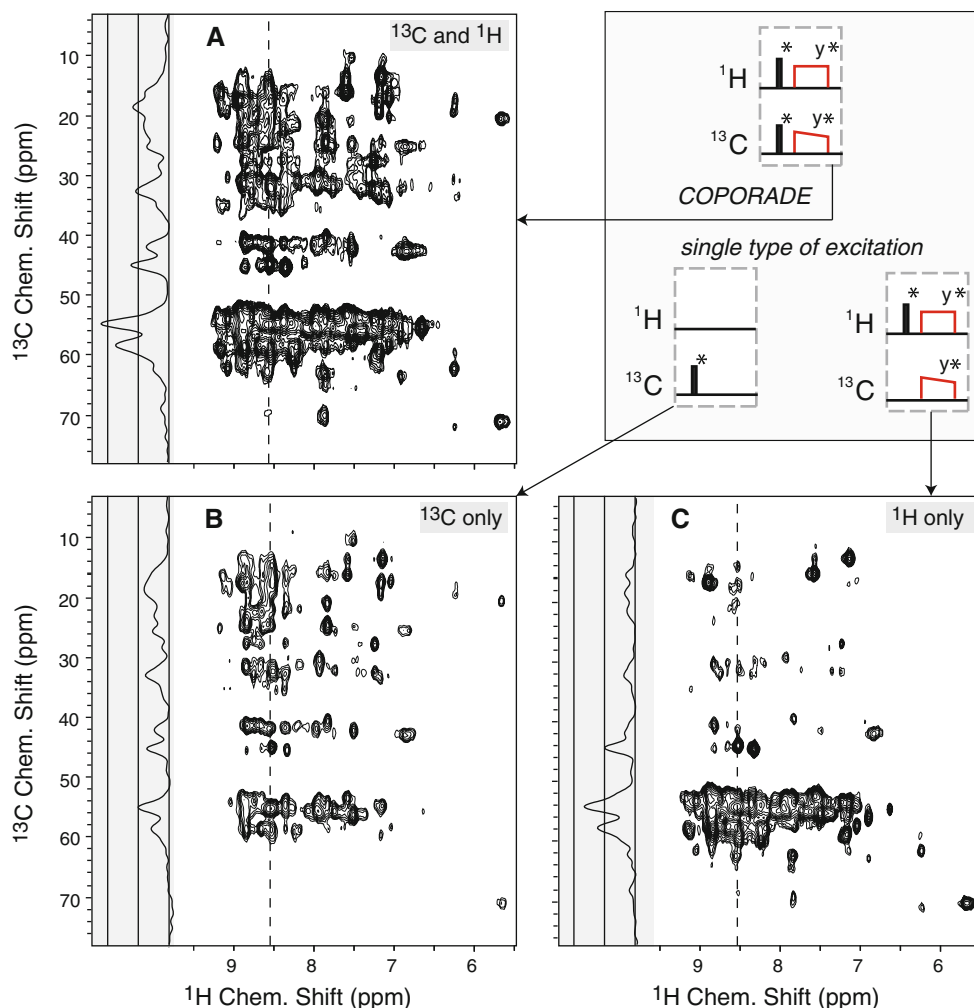


**Fig. 2** Excitation profiles obtained from *COPORADE* (a), direct  $^{13}\text{C}$  excitation only (b), and excitation by long-range transfer from  $^1\text{H}$  only (c), as assessed by  $^{13}\text{C}/^1\text{H}$  2D correlations, recorded within 15 h using  $256 \times 116$  scans (f2xf1) each. The *upper right corner* shows

the type of excitation used for the different experiments, the complete pulse scheme is shown in Supplementary Figure 1B. Traces along the  $^{13}\text{C}$  dimension (on the *left* side of each block) were extracted at a  $^1\text{H}$  chemical shift of 8.55 ppm, as denoted by the *dashed line*

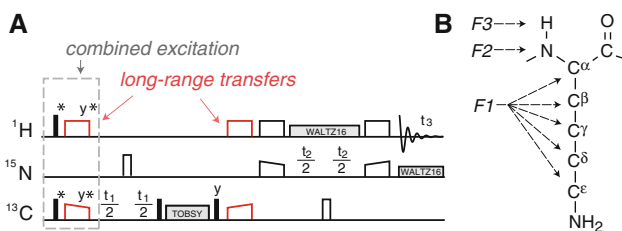


**Fig. 3** Pulse scheme for a side-chain to backbone correlation experiment, using long-range CP transfers (red) and combined  $^1\text{H}/^{13}\text{C}$  excitation (*COPORADE*). These fundamental elements are combined with a CP-based HN-correlation but can in principle be combined with other building blocks, like INEPT-H/N-transfers or water suppression purge pulses, alternatively (see Supplementary Figure 1). The use of a long-range H/C-transfer rather than a direct C/N cross polarization for the transfer of magnetization to the backbone is crucial for all side-chain coherences apart from  $\text{C}^\alpha$  (see Supplementary Figure 7)

build-up of transferred magnetization between the low- $\gamma$  nuclei  $^{13}\text{C}/^{15}\text{N}$  relative to  $^{13}\text{C}/^1\text{H}$ , the need for a much higher power irradiation on a nucleus with a small gyromagnetic ratio for the same effective field provides a hurdle for sensitive samples such as proteins particularly when a long transfer duration is necessary. Although  $^{13}\text{C}$ – $^{13}\text{C}$  mixing by TOBSY (Baldus and Meier 1996), which has been shown to yield correlations among protonated or deuterated side-chain carbons (Agarwal and Reif 2008), was additionally employed for recruiting magnetization from distant carbons (see experimental details in the Supporting Information), lower signal to noise of side-chain correlations was obtained for a direct  $^{13}\text{C}^x$  to  $^{15}\text{N}$  transfer pathway. This confirmed the presumption of an inferior overall transfer efficiency of the C–N–H-route especially for distant side-chain nuclei. (The comparison of the direct C–N–H route versus a “detour” pathway employing long-

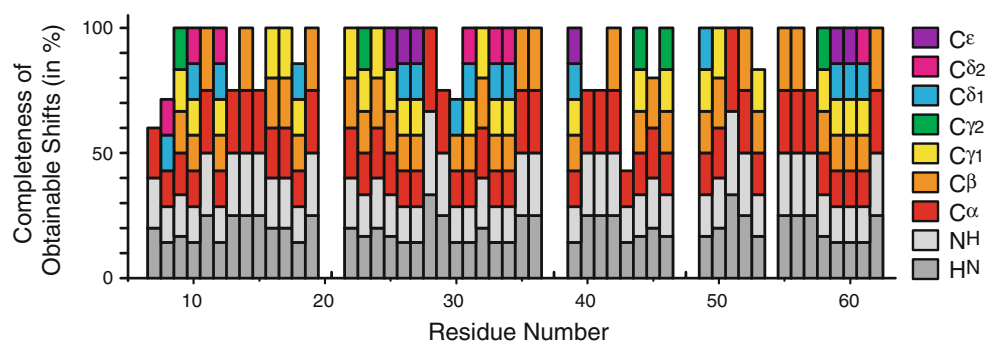


**Fig. 4** Accessible shifts for the SH3 domain of  $\alpha$ -spectrin in a single *S2B* experiment. Shifts that are obscured in the experiment are *left blank*. The height of the *bars* reflects the completeness obtained in each strip of the 3D *S2B*, given by the ratio between the number of shifts actually obtained and the number of shifts that could potentially

be obtained if the strip yielded complete intraresidual correlations. The color coding of the columns accords to which shifts are obtained. Due to the 3D nature of the experiment, at least 3 resonances are obtained whenever a correlation is detected. All residues yielding no correlation signals at all are in highly mobile regions of the protein

distance  $^1\text{H}/^{13}\text{C}$  transfers takes into account the same rf restrictions necessary in order not to dehydrate the protein, in this case maximum CP durations of 4 ms and fields of 50, 50 and 105 kHz for  $^{13}\text{C}$ ,  $^{15}\text{N}$ , and  $^1\text{H}$ , respectively). Similar to alternative mixing sequences (Huang et al. 2011), like  $^{13}\text{C}$  RFDR (Bennett et al. 1992) or DONER (Akbej et al. 2009) for example, the performance of TOBSY is dependent on the number of bonds to traverse (Baldus and Meier 1996). All magnetization remaining on distant carbons after mixing is discarded when a one-bond transfer exclusively from  $\text{C}^\alpha$  is used. These deficiencies result in, at most,  $\text{C}^\beta$  resonances being observed here, with the correlations involving  $\text{C}^\gamma$ ,  $\text{C}^\delta$ , and  $\text{C}^\epsilon$  being below the noise level despite the scalar mixing. A detailed comparison between the indirect transfer with superior performance and the more intuitive direct transfer is represented in Supplementary Figures 7 and 8, with both experiments acquired under identical conditions.

The performance of the 3D side-chain to backbone correlation with the *COPORADE* approach and additional use of long-range  $^1\text{H}/^{13}\text{C}$ -CPs for magnetization transfer to the amide, as obtained with a triple-resonance probe, is assessed quantitatively in the scheme in Fig. 4. Apart from side chains in mobile regions of the SH3 domain (Linsler et al. 2010b) and Pro residues, the *S2B* experiment yields a near complete set of resonances. The number of peaks in generally detectable correlations amount to around 90%. Resonances with intensities below the detection limit are mostly  $\text{C}^\beta$  peaks of aromatic residues. In addition to the intra-residual *S2B* correlations, interresidual ( $i - 1$ ) correlations, mostly for  $\text{C}^\alpha$  resonances, show up in most 3D strips. This is true in particular for Ala and Gly residues with a lower number of side-chain atoms, which show interresidual correlations to  $\text{C}^\beta$  and  $\text{C}^\gamma$  additionally. Tabulation of the chemical shift values obtained for the SH3 domain can be found in the Supplementary Information.

Comparison of the signal to noise of an *S2B* experiment (taking into account the first H/N 2D-plane) with that obtained in a CP-based H/N-correlation of the SH3-domain (using 0.5 s recycle delays) as a reference yields a relative sensitivity of 6.7% based on the number of scans, which results in an effective factor of 3.7% due to the longer recycling delays necessary for the *S2B*.

## Conclusion

Solid-state NMR on perdeuterated samples has been shown to provide NMR spectra for a subset of protein resonances with an extraordinary resolution. Now, for the first time a virtually complete set of resonances including side-chain chemical shifts is shown to be obtainable from a single experiment and one uniformly perdeuterated protein. In particular, this work demonstrates the accessibility of highly resolved correlations between backbone  $\text{H}^\text{N}$  and  $\text{N}^\text{H}$  and the complete set of aliphatic side-chain carbon resonances in addition, which have been difficult to obtain in absence of aliphatic protons. This is achieved by dual polarization through long-range  $^1\text{H}/^{13}\text{C}$  magnetization transfers in addition to PRE-enabled direct carbon excitation. Contradicting the common scope of perdeuteration and its limitations in respect to side-chain nuclei, this work indicates that proton-detected solid-state NMR is not merely an exotic addition to traditional methods based on protonated samples anymore, but rather represents a potent source for diverse NMR data beneficial for side-chain dynamics and mapping of binding events.

**Acknowledgments** I am grateful to Prof. Bernd Reif for fruitful and very helpful discussions. Dr. James Hook is kindly acknowledged for his support to the project. This research was financed by the Analytical Centre, UNSW.

## References

- Agarwal V, Reif B (2008) Residual methyl protonation in perdeuterated proteins for multi-dimensional correlation experiments in MAS solid-state NMR spectroscopy. *J Magn Reson* 194:16–24
- Agarwal V, Linser R, Fink U, Faelber K, Reif B (2010a) Identification of hydroxyl protons, determination of their exchange dynamics, and characterization of hydrogen bonding by MAS solid-state NMR spectroscopy in a microcrystalline protein. *J Am Chem Soc* 132:3187–3195
- Agarwal V, Linser R, Fink U, Fälber K, Reif B (2010b) Identification of hydroxyl protons and characterization of exchange behaviour and hydrogen bonding in a microcrystalline protein. *J Am Chem Soc* 132:3187–3195
- Akbej U, Oschkinat H, van Rossum B (2009) Double-nucleus enhanced recoupling for efficient  $^{13}\text{C}$  MAS NMR correlation spectroscopy of perdeuterated proteins. *J Am Chem Soc* 131:17054–17055
- Asami S, Schmieder P, Reif B (2010) High resolution  $^1\text{H}$ -detected solid-state NMR spectroscopy of protein aliphatic resonances: access to tertiary structure information. *J Am Chem Soc* 132:15133–15135
- Baldus M, Meier BH (1996) Total correlation spectroscopy in the solid state. The use of scalar couplings to determine the through-bond connectivity. *J Magn Reson* 121:65–69
- Bennett AE, Ok JH, Vega S, Griffin RG (1992) Chemical shift correlation spectroscopy in rotating solids: radio frequency-driven dipolar recoupling and longitudinal exchange. *J Chem Phys* 96:8624–8627
- Cady SD et al (2010) Structure of the amantadine binding site of influenza M2 proton channels in lipid bilayers. *Nature* 463:689–692
- Castellani F et al (2002) Structure of a protein determined by solid-state magic-angle-spinning NMR spectroscopy. *Nature* 420:98–102
- Chevelkov V, Rehbein K, Diel A, Reif B (2006) Ultra-high resolution in proton solid-state NMR spectroscopy at high levels of deuteration. *Angew Chem Int Ed* 45:3878–3881
- Chevelkov V, Fink U, Reif B (2009) Accurate determination of order parameters from  $^1\text{H}$ ,  $^{15}\text{N}$  dipolar couplings in MAS solid-state NMR experiments. *J Am Chem Soc* 131:14018–14022
- Chevelkov V, Xue Y, Linser R, Skrynnikov N, Reif B (2010) Comparison of solid-state dipolar couplings and solution relaxation data provides insight into protein backbone dynamics. *J Am Chem Soc* 132:5015–5017
- Goddard TD, Kneller DG (2004) SPARKY 3, University of California, San Francisco
- Huang KY, Siemer AB, McDermott AE (2011) Homonuclear mixing sequences for perdeuterated proteins. *J Magn Reson* 208:122–127
- Lange A et al (2006) Toxin-induced conformational changes in a potassium channel revealed by solid-state NMR. *Nature* 440:959–962
- Leppert J, Ohlenschläger O, Groll M, Ramachandran R (2004) Adiabatic TOBSY in rotating solids. *J Biomol NMR* 29:167–173
- Linser R, Chevelkov V, Diehl A, Reif B (2007) Sensitivity enhancement using paramagnetic relaxation in MAS solid-state NMR of perdeuterated proteins. *J Magn Reson* 189:209–216
- Linser R, Fink U, Reif B (2008) Proton-detected scalar coupling based assignment strategies in MAS solid-state NMR spectroscopy applied to perdeuterated proteins. *J Magn Reson* 193:89–93
- Linser R, Fink U, Reif B (2009) Probing surface accessibility of proteins using paramagnetic relaxation in solid-state NMR spectroscopy. *J Am Chem Soc* 131:13703–13708
- Linser R, Fink U, Reif B (2010a) Narrow carbonyl resonances in proton-diluted proteins facilitate NMR assignments in the solid state. *J Biomol NMR* 47:1–6
- Linser R, Fink U, Reif B (2010b) Assignment of dynamic regions in biological solids enabled by spin-state selective NMR experiments. *J Am Chem Soc* 132:8891–8893
- Linser R, Bardiaux B, Higman V, Fink U, Reif B (2011a) Structure calculation from unambiguous long-range amide and methyl  $^1\text{H}$ - $^1\text{H}$  distance restraints for a micro-crystalline protein with MAS solid state NMR. *J Am Chem Soc* 133:5905–5912
- Linser R et al (2011b) Proton detected solid-state NMR of fibrillar and membrane proteins. *Angew Chem Int Ed* 50:4508–4512
- Loquet A et al (2008) 3D structure determination of the Crh protein from highly ambiguous solid-state NMR restraints. *J Am Chem Soc* 130:3579–3589
- Loria JP, Rance M, Palmer AG (1999) A relaxation-compensated Carr-Purcell-Meiboom-Gill sequence for characterizing chemical exchange by NMR spectroscopy. *J Am Chem Soc* 121:2331–2332
- McDermott AE, Creuzet FJ, Kolbert AC, Griffin RG (1992) High-resolution magic-angle-spinning NMR spectra of protons in deuterated solids. *J Magn Reson* 98:408–413
- Morcombe CR, Paulson EK, Gaponenko V, Byrd RA, Zilm KW (2005)  $^1\text{H}$ - $^{15}\text{N}$  correlation spectroscopy of nanocrystalline proteins. *J Biomol. NMR* 31:217–230
- Petkova AT et al (2002) A structural model for Alzheimer's  $\beta$ -amyloid fibrils based on experimental constraints from solid state NMR. *Proc Natl Acad Sci USA* 99:16742–16747
- Pintacuda G, Otting G (2002) Identification of protein surfaces by NMR measurements with a paramagnetic Gd(III) chelate. *J Am Chem Soc* 124:457–471
- Schanda P, Huber M, Verel R, Ernst M, Meier BH (2009) Direct detection of  $^3\text{H}_{\text{NC}}$  hydrogen-bond scalar couplings in proteins by Solid-state NMR spectroscopy. *Angew Chem Int Ed* 48:9322–9325
- Schanda P, Meier BH, Ernst M (2010) Quantitative analysis of protein backbone dynamics in microcrystalline ubiquitin by solid-state NMR spectroscopy. *J Am Chem Soc* 132:15957–15967
- Sprangers R, Kay LE (2008) Quantitative dynamics and binding studies of the 20S proteasome by NMR. *Nature* 445:618–622
- Tang M, Comellas G, Mueller LJ, Rienstra CM (2010) High resolution  $^{13}\text{C}$ -detected solid-state NMR spectroscopy of a deuterated protein. *J Biomol NMR* 48:103–111
- Velyvis A, Schachman HK, Kay LE (2009) Assignment of Ile, Leu, and Val Methyl correlations in supra-molecular systems: an application to aspartate transcarbamoylase. *J Am Chem Soc* 131:16534–16543
- Vranken WF et al (2005) The CCPN data model for NMR spectroscopy: development of a software pipeline. *Proteins* 59:687–696
- Wasmer C et al (2008) Amyloid fibrils of the HET-s(218–289) prion form a beta solenoid with a triangular hydrophobic core. *Science* 319:1523–1526
- Wickramasinghe NP, Kotecha M, Samoson A, Paast J, Ishii Y (2007) Sensitivity enhancement in  $^{13}\text{C}$  solid-state NMR of protein microcrystals by use of paramagnetic metal ions for optimizing  $^1\text{H}$  T1 relaxation. *J Magn Reson* 184:350–356
- Wittekind M, Mueller L (1993) HNCACB: a high sensitivity 3D NMR experiment to correlate amide proton and nitrogen resonances with the  $\alpha$ -carbon and  $\beta$ -carbon resonances in proteins. *J Magn Reson* B101